[CANCER RESEARCH 64, 8674–8681, December 1, 2004]

Integrin Fibronectin Receptors in Matrix Metalloproteinase-1–Dependent Invasion by Breast Cancer and Mammary Epithelial Cells

Yifeng Jia, Zhao-Zhu Zeng, Sonja M. Markwart, Korrene F. Rockwood, Kathleen M. Woods Ignatoski, Stephen P. Ethier, and Donna L. Livant

Department of Radiation Oncology and Comprehensive Cancer Center, University of Michigan, Ann Arbor, Michigan

ABSTRACT

Integrins contribute to progression in many cancers, including breast cancer. For example, the interaction of $\alpha_5\beta_1$ with plasma fibronectin causes the constitutive invasiveness of human prostate cancer cells. Inhibition of this process reduces tumorigenesis and prevents metastasis and recurrence. In this study, naturally serum-free basement membranes were used as invasion substrates. Immunoassays were used to compare the roles of $\alpha_5\beta_1$ and $\alpha_4\beta_1$ fibronectin receptors in regulating matrix metalloproteinase (MMP)-1–dependent invasion by human breast cancer and mammary epithelial cells. We found that a peptide consisting of fibronectin PHSRN sequence, Ac-PHSRN-NH_2, induces $\alpha_5\beta_1$-mediated invasion of basement membranes *in vitro* by human breast cancer and mammary epithelial cells. PHSRN-induced invasion requires interstitial collagenase MMP-1 activity and is suppressed by an equimolar concentration of a peptide consisting of the LDV sequence of the fibronectin connecting segment, Ac-LHGPEILDVPST-NH_2, in mammary epithelial cells, but not in breast cancer cells. This sequence interacts with $\alpha_4\beta_1$, an integrin that is often down-regulated in breast cancer cells. Immunoblotting shows that the PHSRN peptide stimulates MMP-1 production by serum-free human breast cancer and mammary epithelial cells and that the LDV peptide represses PHSRN-stimulated MMP-1 production only in mammary epithelial cells. Furthermore, PHSRN stimulates MMP-1 activity in breast cancer cells and mammary epithelial cells with a time course that closely parallels invasion induction. Thus, down-regulation of surface $\alpha_4\beta_1$ during oncogenic transformation may be crucial for establishment of the $\alpha_5\beta_1$-induced, MMP-1–dependent invasive phenotype of breast cancer cells.

INTRODUCTION

Integrins are a family of α/β heterodimeric receptors that mediate cell–matrix and cell–cell interactions and have important functions in cell migration, survival, and differentiation (reviewed in refs. 1 and 2). In addition to functioning in cellular adhesion to the extracellular matrix, integrins are known to mediate many diverse processes involving cell migration and invasion. For example, the $\alpha_5\beta_1$ fibronectin receptor has been shown to play a key role in wound healing by mediating invasion of the provisional matrix by fibroblasts, endothelial cells, and keratinocytes to accomplish angiogenesis and re-epithelialization (3, 4). Also, integrins have been shown to function in the progression of a variety of cancers (reviewed in ref. 5).

One very important way that integrins can contribute to cancer progression is to mediate cancer cell invasion, thus causing metastasis. For example, we have shown that the interaction of plasma fibronectin (pFn) with $\alpha_5\beta_1$ integrin induces human prostate cancer cell invasion (6–8) by using the naturally serum-free (SF), selectively permeable (9) basement membranes of sea urchin embryos [sea urchin embryo basement membranes with extracellular matrix (SU-ECM)] as *in vitro* invasion substrates (10). Even in the presence of serum, SU-ECM have been shown to be free of background invasion by unstimulated normal cells (3, 6, 10), which can be observed when artificial or reconstituted basement membranes are used (11). Also, these basement membranes are similar to those of mammals, both structurally and functionally (12–14). Because they are naturally SF, we used SU-ECM to identify PHSRN as the specific sequence of pFn that interacts with $\alpha_5\beta_1$ to stimulate invasion by human prostate cancer cells and to show that inhibition of pFn-induced invasion reduces tumorigenesis and prevents metastasis and recurrence in both rat and human preclinical models of prostate cancer (6, 7).

Because fibronectin is found throughout the body, the proper regulation of $\alpha_5\beta_1$-mediated collagenase expression, and hence invasion, is very important. This is accomplished by another integrin fibronectin receptor, $\alpha_4\beta_1$. When fibronectin is intact, $\alpha_4\beta_1$ integrin interacts with the LDV sequence of the fibronectin connecting segment, LHGPEILDVPST, to repress $\alpha_5\beta_1$-mediated interstitial collagenase expression in adherent fibroblasts (15). Fragmentation of fibronectin by plasmin has been shown to de-repress $\alpha_5\beta_1$-mediated invasion during wound healing (16, 17); thus, an important attribute of $\alpha_5\beta_1$-induced invasion in normal cells is its regulation by $\alpha_4\beta_1$ integrin.

Although still expressing abundant surface $\alpha_5\beta_1$, metastatic prostate and breast cancer cells have low levels of surface $\alpha_4\beta_1$, relative to prostate and mammary epithelial cells (18, 19). Loss of surface $\alpha_4\beta_1$, which can result from oncogene overexpression in transformed mammary epithelial cells (19), causes constitutive invasiveness in the presence of the abundant pFn of blood, lymph, and interstitial fluid (20, 21). Because of its importance in breast cancer cell invasion and metastasis, we undertook this study to define the receptor–ligand interaction responsible for the invasive phenotype of metastatic breast cancer cells and to assess the role of interstitial collagenase matrix metalloproteinase (MMP)-1 in basement membrane invasion *in vitro*.

MATERIALS AND METHODS

Cell Culture. SUM-52 PE and MCF-10A cells were cultured in SF media, as described previously (22); whereas 5% serum was present in cultured SUM-149 PT and normal human mammary epithelial (HME) cells (23). When necessary, SUM-149 PT cells were serum-starved overnight before the addition of peptides.

Peptide Synthesis. NH_2-terminal acetylated, COOH-terminal amidated PHSRN and LDV peptides (Ac-PHSRN-NH_2 andAc-LHGPEILDVPST-NH_2), their randomized sequence controls (Ac-HSPNR-NH_2 and Ac-PGVLSEHPTLID-NH_2), RGD peptide (Ac-GRGDSP-NH_2), and VKNEED peptide (Ac-VKNEED-NH_2) were synthesized using Fmoc/*t*-butyl-9-fluorenylmethoxycarbonyl/*t*-butyl protection strategies (24) at 25- and 100-μm scales on a Ranin Symphony peptide synthesizer. COOH-terminally amidated peptides were synthesized on Rink resin. Anhydrous trifluoroacetic acid was used to remove side chain protecting groups and to cleave peptides from the resin support. Peptides were precipitated with diethylether, purified by preparative

Received 1/9/04; revised 8/24/04; accepted 9/29/04.

Grant support: A research grant from Attenuon, L.L.C. (D. Livant) and National Cancer Institute R01 grant CA 70354 (S. Ethier).

The costs of publication of this article were defrayed in part by the payment of page charges. This article must therefore be hereby marked *advertisement* in accordance with 18 U.S.C. Section 1734 solely to indicate this fact.

Note: Y. Jia is currently in the Laboratory of Pathology, Center for Cancer Research, National Cancer Institute, National Institutes of Health, Bethesda, Maryland. S. Ethier is currently in the Barbara Ann Karmanos Cancer Institute, Wayne State University, Detroit, Michigan.

Requests for reprints: Donna L. Livant, Department of Radiation Oncology, Room 3007, 1331 East Ann Street Building, Ann Arbor, MI 48109-0582. Phone: 734-764-0313; Fax: 734-763-1581; E-mail: dlivant@umich.edu.

high-performance liquid chromatography, and lyophilized. Peptide purities were assessed by reverse-phase high-performance liquid chromatography and found to be 95% for Ac-PHSRN-NH_2, 97% for Ac-HSPNR-NH_2, 93% for Ac-LHGPEILDVPST-NH_2, 92% for Ac-PGVLSEHPTLID-NH_2, 95% for Ac-GRGDSP-NH_2, and 91% for Ac-VKNEED-NH_2 (data not shown). Peptide structures were confirmed by mass spectrometry and amino acid analysis (data not shown) using standard methods (24). Residual trifluoroacetic acid was removed by gel permeation chromatography on Sephadex G-10 in 1 N acetic acid. Peptides were lyophilized and stored in the presence of a desiccant at −30°C until solubilization in phosphate-buffered saline at 1 mg/mL at the time of use.

Antibodies Used in Invasion Assays. P1D6 anti-$\alpha_5\beta_1$ or P1B5 anti-$\alpha_3\beta_1$ integrin function-blocking monoclonal antibodies (mAbs) (25, 26), from Oncogene Research Products (Boston, MA), were prebound to suspended cells in SF or fetal calf serum (FCS)-containing media on ice for 30 minutes at 10 to 300 μg/mL before 10-fold dilution in the appropriate medium and placement on SU-ECM. P1H4 and P4C2 function-blocking anti-$\alpha_4\beta_1$ integrin mAbs (27, 28), from Chemicon International (Temecula, CA), were prebound to cells, and the cells were used in invasion assays as described above. Function-blocking anti–MMP-1 (COMY-4A2), anti–MMP-2 (CA-4001), and anti–MMP-9 (GE-213) mAbs (29–31) from Chemicon International were prebound to cells, and the cells used in invasion assays as described above. Isotype control antibodies were as follows: IgM (BD Biosciences PharMingen, San Diego, CA); and IgG1 and IgG3 (Sigma, St. Louis, MO). All isotype control antibodies were prebound to cells, and the cells were used in invasion assays as described above.

Invasion Assays. Preparation of SU-ECM and *in vitro* SU-ECM invasion assays were performed with or without added FCS, as described previously (3, 6, 10). Plasma fibronectin-depleted (pFn$^-$) FCS was made using gelatin affinity chromatography, as described previously (6, 19, 21). Single-cell suspensions were made with 0.25% trypsin/EDTA (Gibco Life Technologies, Inc., Grand Island, NY). Cell suspensions were rinsed by pelleting and resuspension in the appropriate medium before placement on SU-ECM invasion substrates. Invasion percentages and cellular viabilities were scored as described previously (3, 6, 10, 19). Peptides were added to the invasion assays by prebinding to suspended, rinsed cells for 5 minutes at room temperature. For assays demonstrating anti–MMP-1 inhibition of PHSRN-induced invasion, the concentration of Ac-PHSRN-NH_2 in the assay medium was 1 μg/mL. Antibodies were prebound to suspended cells, as described above. Each invasion percentage is the ratio of the total number of single cells located in the interior, blastocoelic cavities of the SU-ECM substrates to the total number of single cells adhering to both their exterior and interior surfaces, and is the result of three to four independent determinations involving the scoring of the positions of all individual cells adhering to the SU-ECM invasion substrates.

Fluorescence-Activated Cell Sorting. Fluorescence-activated cell sorting of SUM-52 PE and MCF-10A cells was performed as described previously (19), using anti-integrin α_4 antibody (catalog no. 12077-012; Gibco) or anti-integrin α_5 antibody (catalog no. CP12L; Oncogene Research Products) followed by fluorescein-conjugated donkey antimouse IgG (1:100; Chemicon International). Negative controls contained cells bound to fluorescein-conjugated donkey antimouse IgG without primary antibody.

SDS-PAGE and Immunoblotting. Each sample contained 2×10^6 adherent cells treated with the appropriate peptides for 16 hours at 37°C. The treatment groups were as follows: SF medium only; SF medium + Ac-PHSRN-NH_2; SF medium + Ac-LHGPEILDVPST-NH_2; SF medium + Ac-PHSRN-NH_2 + Ac-LHGPEILDVPST-NH_2; and SF medium + Ac-PHSRN-NH_2 + Ac-PGVLSEHPTLID-NH_2. All cells were rinsed, and 5 mL of fresh SF medium were added to each sample before peptide addition. Samples were treated as follows: 1 μg of Ac-PHSRN-NH_2 per 20,000 cells (100 μg for 2×10^6 cells in 5 mL of medium); 2.5 μg of Ac-LHGPEILDVPST-NH_2 per 20,000 cells; 1 μg of Ac-PHSRN-NH_2 and 2.5 μg of Ac-LHGPEILDVPST-NH_2 per 20,000 cells; or 1 μg of Ac-PHSRN-NH_2 and 2.5 μg of Ac-PGVLSEHPTLID-NH_2 per 20,000 cells.

SUM-52 PE, SUM-149 PT, and MCF-10A cells were rinsed with PBS and lysed in ice-cold buffer [50 mmol/L Tris-HCI (pH 7.5), 150 mmol/L NaCl, 2 mmol/L EGTA, and 1% Triton X-100] containing protease inhibitors (1× complete protease inhibitor mixture; Roche, Indianapolis, IN). The lysate was collected and centrifuged at 12,000 × *g* for 10 minutes at 4°C, and the resulting pellet was resuspended in SDS sample buffer [2% SDS, 62.5 mmol/L Tris-HCI (pH 6.8), and 10% glycerol]. The amounts of protein were measured for each sample using the Bio-Rad protein assay kit (catalog no. 500-0006; Bio-Rad, Richmond, CA) with albumin standards. Before electrophoresis, samples were brought to 5% (v/v) 2-mercaptoethanol and boiled for 5 minutes.

To verify a rapid increase in latent and activated MMP-1 secreted into the SF medium after Ac-PHSRN-NH_2 treatment, adherent cultures of 2×10^6 SUM-52 PE or SUM-149 PT breast cancer cells and 2×10^6 MCF-10A mammary epithelial cells in SF medium were treated with 1 μg of Ac-PHSRN-NH_2 per 20,000 cells (100 μg in 5 mL of medium) for periods of time ranging from 1 hour to 6 hours. Media were collected and concentrated 50-fold using centrifugal filter devices (Amicon Ultra PL-10 device; 10,000 nominal molecular weight limit; Millipore, Bedford, MA), according to the manufacturer's instructions. The quantitative consistency of the volume reduction was verified by using a micropipetting device for all media assayed.

For cell lysates, 30 μg of total protein per sample in SDS buffer were resolved on 10% polyacrylamide gels using a mini-PROTEAN II Electrophoresis Cell (Bio-Rad, Hercules, CA). Separated proteins were transferred onto polyvinylidene difluoride membranes (Milllipore) using the submarine electrophoretic transfer unit in the same apparatus. Varying amounts (10, 5, 2.5, and 1.25 ng) of recombinant MMP-1 (catalog no. CC1031; Chemicon International) were combined with cytoskeletal actin and loaded on the same gel for generation of standard curves. Membranes were blocked for 1 hour in 0.1% (v/v) Tween 20 in PBS (PBS-T) containing 5% (w/v) nonfat dry milk and then incubated for 1 hour at room temperature with anti–MMP-1 mAb (clone COMY-4A2; Chemicon International) at a 1:5,000 dilution in blocking solution.

For the analysis of secreted MMP-1 levels by immunoblotting, identical volumes of concentrated media from PHSRN-treated and untreated cells were run on 10% polyacrylamide gels, as described above. Recombinant MMP-1 was diluted 3,000-fold and run in varying amounts on each gel as positive controls. Separated proteins were transferred onto polyvinylidene difluoride membranes as described above, and membranes were incubated overnight at 4°C with rabbit anti–MMP-1 polyclonal antibody (catalog no. AB806, Chemicon International) at a dilution of 1:1,000 in Tris-buffered saline with 0.05% Tween 20.

After incubation with the primary antibody, all membranes were washed three times in PBS-T and incubated for 1 hour with goat antimouse IgG antibody conjugated to horseradish peroxidase (Jackson Immunoresearch Laboratories, West Grove, PA) at a dilution of 1:5,000 in blocking solution. The membranes were then washed three times in PBS-T and processed for detection by enhanced chemiluminescence ECL reagent (Amersham, Arlington Heights, IL). The amounts of MMP-1 and actin from the cell lysates were quantified using Quantity One software (Bio-Rad, Hercules, CA) by comparison with the recombinant MMP-1 and actin standard curves generated from the same blot. Then, the amount of MMP-1 was normalized to the amount of total cellular actin in each sample from cell lysates. In immunoblots used to compare MMP-1 levels in the media of PHSRN-treated and untreated cells, equal volumes of concentrated media were loaded without normalization of protein content.

Matrix Metalloproteinase-1 Activity Assay. Adherent SUM-149 PT, SUM-52 PE, or MCF-10A cells were treated for various times with Ac-PHSRN-NH_2 at a concentration of 1 μg per 20,000 cells in SF medium, and untreated controls were performed in parallel. Culture media were concentrated 10-fold by centrifugation through Centricon YM-10 filter units (Fisher Scientific Company, L.L.C., Pittsburgh, PA), according to the manufacturer's instructions. The quantitative consistency of the volume reduction was verified by using a micropipetting device for all media assayed. MMP-1 activity was measured in concentrated media with the Biotrak MMP-1 activity assay system (Amersham Pharmacia Biotech Inc., Piscataway, NJ), according to the manufacturer's instructions. The assays were read at 405 nm in a microtiter plate spectrophotometer (Dynatech Laboratories, Inc., Chantilly, VA). A standard curve was generated from a set of known aliquots of MMP-1 in the following concentration range: 0, 0.10, 0.20, 0.40, 0.80, and 1.60 ng/mL. Each time point was assayed at least three times in triplicate, and mean MMP-1 activities were determined with their first SDs. The results were analyzed using Student's *t* test.

RESULTS

Invasion Induction by the PHSRN Peptide. The effects of the PHSRN peptide on invasion by HME and MCF-10A mammary epithelial cells and SUM-149 PT and SUM-52 PE breast cancer cells were evaluated on SU-ECM invasion substrates. As shown in Fig. 1*A*, the blocked PHSRN peptide stimulated invasion by HME with a log-linear dose-response relationship at concentrations from 10 ng/mL to 1 μg/mL (17 nmol/L to 1.7 μmol/L), whereas the scrambled, blocked PHSRN peptide, Ac-HSPNR-NH_2, was without detectable activity at 17 μmol/L. In addition to PHSRN (32), $\alpha_5\beta_1$ interacts with the RGD (8) and VKNEED sequences of the fibronectin cell binding domain (33). Thus, the acetylated, amidated derivatives of these peptides were also tested for invasion induction. As shown in Fig. 1*A*, neither GRGDSP nor VKNEED induced HME invasion at concentrations as high as 10 μg/mL. Very similar results were obtained for MCF-10A cells (Fig. 1*B*). In addition, the PHSRN peptide was equally effective at stimulating invasion by MCF-10A and HME cells, irrespective of the presence of FCS. Furthermore, no invasion occurred in the absence of the PHSRN peptide, either in SF medium or in the presence of FCS (data not shown).

Under SF conditions, the PHSRN peptide was equally effective at stimulating invasion by SUM-149 PT breast cancer cells, whereas the HSPNR, RGD, and VKNEED peptides lacked activity, as shown in Fig. 1*C*. Quantitatively similar results were obtained for SUM-52 PE breast cancer cells in SF medium, as shown in Fig. 1*D*. Thus, the PHSRN peptide was as effective at stimulating invasion by MCF-10A and HME cells as it was at stimulating invasion by SF SUM149-PT and SUM 52-PE breast cancer cells.

Induction of Plasma Fibronectin-Dependent Invasion in Mammary Epithelial Cells by Anti-$\alpha_4\beta_1$ Antibody. Because loss of surface $\alpha_4\beta_1$ causes a pFn-dependent, constitutively invasive phenotype in SUM-149 PT cells (19), we tested the whether blocking $\alpha_4\beta_1$ could render mammary epithelial cells invasive in the presence of serum. Levels of surface $\alpha_5\beta_1$ and $\alpha_4\beta_1$ are shown for mammary epithelial and breast cancer cells in Table 1. Like HME, MCF-10A cells express relatively high levels of surface $\alpha_5\beta_1$ and $\alpha_4\beta_1$. In contrast, whereas SUM-52 PE and SUM-149 PT cells express abundant surface $\alpha_5\beta_1$, fluorescence-activated cell-sorting analysis shows that they express very low levels of $\alpha_4\beta_1$.

Table 1 *Cell surface integrin expression*

Cell line	α_4 *	α_5 *
HME †	54	62
MCF-10A	58	30
SUM-52 PE	5	28
SUM-149 PT †	0	10

NOTE. As determined by fluorescence-activated cell-sorting analysis.
* Percentage increase in the amount staining over negative control.
† Data from ref. 19.

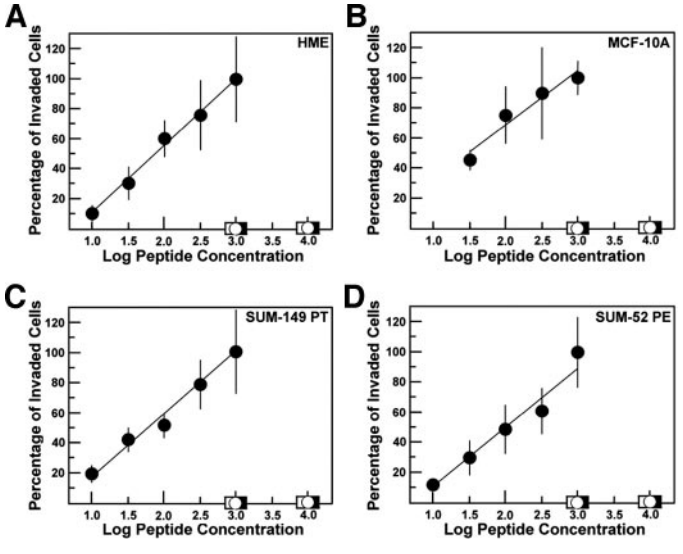

Fig. 1. $\alpha_5\beta_1$-Mediated invasion induced by the blocked PHSRN peptide, Ac-PHSRN-NH_2. *A*, HME cells; *B*, MCF-10A cells; *C*, SUM-149 PT cells; *D*, SUM-52 PE cells. *X axes*, log peptide concentration (in ng/mL). *Y axes*, mean percentages of invasive cells, relative to invasion percentages observed in positive controls (invasion assays containing1 μg/mL PHSRN and performed in parallel). ●, Ac-PHSRN-NH_2–treated cells; ○, Ac-HSPNR-NH_2–treated cells; ■, Ac-GRGDSP-NH_2–treated cells; □, Ac-VKNEED-NH_2–treated cells. *Vertical bars*, first SDs.

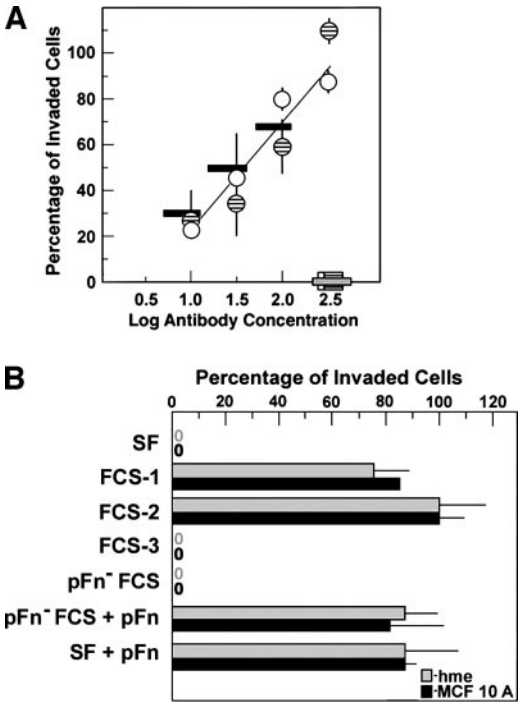

Fig. 2. Blocking anti-$\alpha_4\beta_1$ mAb induces pFn-dependent mammary epithelial cell invasion. *A*. P1H4 and P4C2 mAbs induce mammary epithelial cell invasion in FCS-containing medium. *X axis*, log antibody concentration (in μg/mL). *Y axis*, mean percentage of invasive cells, relative to positive controls containing 1 μg/mL Ac-PHSRN-NH_2. Invasion by either HME or MCF-10A cells did not occur in the absence of anti-$\alpha_4\beta_1$ mAb. ○, HME cells bound to purified P1H4 mAb; ⛀, MCF-10A cells bound to purified P1H4 mAb; ■, HME cells bound to P4C2 ascites fluid; □, HME cells bound to P1H4 isotype control; ▤, MCF-10A cells bound to P1H4 isotype control; ▨, HME cells bound to P4C2 isotype control. Symbols ■ and ▨ reflect the mAb concentration range of the P4C2 ascites fluid. *Vertical bars*, first SDs. *B*, dependence of P4C2 anti-$\alpha_4\beta_1$–induced invasion on pFn. *X axis*, mean percentages of invasive cells, relative to positive controls performed in parallel: percentage of invasive cells in the presence of FCS after binding to 100 μg/mL P4C2 mAb. *Y axis*, media components. ▨ and *gray 0*, HME; ■ and *black 0*, MCF-10A cells. *SF*, SF invasion assay medium; *FCS-1*, 5% FCS in invasion assay medium, P4C2 prebound in SF medium; *FCS-2*, 5% FCS in invasion assay medium and during P4C2 prebinding; *FCS-3*, 5% FCS in invasion assay medium and during isotype control prebinding; *pFn⁻ FCS*, fibronectin-depleted FCS in invasion assay medium and in P4C2 prebinding; *pFn*, 4 μg/mL pFn in SF medium in invasion assays and in P4C2 prebinding. *Vertical bars*, first SDs.

To assess the role of $\alpha_4\beta_1$ in repressing serum-induced invasion, HME and MCF-10A cells were treated with blocking anti-$\alpha_4\beta_1$ mAb before placement on SU-ECM invasion substrates. Fig. 2*A* shows the relative percentages of invasive HME and MCF-10A when the cells were prebound with increasing amounts of P1H4 or P4C2 blocking anti-$\alpha_4\beta_1$ mAb (27, 28). Both P4C2 and P1H4 mAbs stimulated SU-ECM invasion by HME and MCF-10A cells in the presence of FCS, whereas their corresponding isotype control antibodies did not.

Because the P4C2 epitope specifically includes the region of $\alpha_4\beta_1$ that binds the LDV sequence (28, 34) to repress $\alpha_5\beta_1$-mediated

MMP-1 expression (15), the P4C2 mAb was tested for its ability to stimulate SU-ECM invasion by HME and MCF-10A cells while the presence of FCS and/or pFn was varied systematically in the media of the invasion assays. Antibody prebinding occurred in either SF medium, FCS-containing medium, or pFn-depleted FCS-containing medium, as indicated. As shown for HME and MCF-10A in Fig. 2*B*, the P4C2 anti-$\alpha_4\beta_1$ mAb was unable to stimulate invasion in SF medium, but it stimulated invasion by HME and MCF-10A cells in FCS-containing medium. Also, P4C2-stimulated invasion was specifically dependent on pFn because no invasion occurred if P4C2-bound HME or MCF-10A cells were incubated on SU-ECM substrates in pFn^- FCS. The addition of 4 μg/mL pFn, the concentration found in 10% FCS (20, 21), to medium containing pFn^- FCS (pFn^- FCS + pFn) restored the ability of the P4C2 mAb to stimulate HME and MCF-10A invasion. Also, the addition of 4 μg/mL pFn to SF medium (SF + pFn) was sufficient to permit P4C2-induced invasion. Thus, pFn appeared to be both necessary and sufficient for P4C2 anti-$\alpha_4\beta_1$–induced invasion by both HME and MCF-10A cells.

Repression of PHSRN-Induced Invasion by the LDV Sequence. An acetylated, amidated peptide containing the LDV sequence (Ac-LHGPEILDVPST-NH_2) was tested for its ability to repress PHSRN-induced invasion by normal and neoplastic breast epithelial cells. Because a single copy of each sequence is found in the fibronectin monomer (32, 34), the PHSRN and LDV peptides were tested at equimolar concentrations. Fig. 3*A* shows that whereas PHSRN stimulated HME invasion of the SU-ECM, the presence of an equimolar concentration of the LDV peptide prevented PHSRN-induced invasion. Furthermore, inhibition was sequence specific because the scrambled LDV peptide (Ac-PGVLSEHPTLID-NH_2) had no inhibitory effect on PHSRN-induced invasion. Analogous results were obtained for MCF-10A cells (Fig. 3*B*). Thus, the ability of the LDV peptide to inhibit PHSRN-induced HME and MCF-10A invasion is consistent with the expression of abundant surface $\alpha_5\beta_1$ and $\alpha_4\beta_1$ fibronectin receptors by these cells (ref. 19 and this study). In contrast, as shown in Fig. 3*C* and *D*, the LDV peptide had no inhibitory effect on PHSRN-induced invasion by either SUM-149 PT or SUM-52 PE cells. The failure of the LDV sequence to inhibit PHSRN-induced SUM-149 PT and SUM-52 PE invasion is likewise consistent with the expression of surface $\alpha_5\beta_1$, but not $\alpha_4\beta_1$, by these breast cancer cell lines.

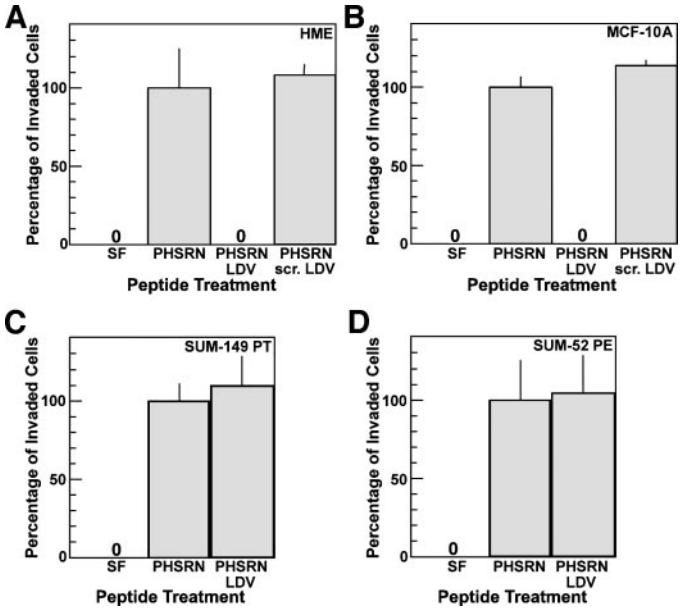

Fig. 3. Repression of PHSRN-induced mammary epithelial cell but not breast cancer cell invasion by the blocked LDV peptide. *A*, HME cells; *B*, MCF-10A cells; *C*, SUM-149 PT cells; *D*, SUM-52 PE cells. *X axes*, peptide treatment. *Y axes*, percentage of invasive cells. Mean percentages of invasive cells, relative to mean percentages of invasive cells in the presence of 100 ng/mL Ac-PHSRN-NH_2 (in SF medium), are plotted. Media components were as follows: *SF*, no peptide in SF medium; *PHSRN*, 100 ng/mL Ac-PHSRN-NH_2 in SF medium; *PHSRN LDV*, 100 ng/mL Ac-PHSRN-NH_2 and 250 ng/mL Ac-LHGPEILDVPST-NH_2 in SF medium; *PHSRN scr. LDV*, 100 ng/mL Ac-PHSRN-NH_2 and 250 ng/mL Ac-PGVLSEHPTLID-NH_2 in SF medium. *Vertical bars*, first SDs.

Role of Matrix Metalloproteinase-1 in $\alpha_5\beta_1$-Mediated Invasion. The role of MMP-1 in PHSRN-induced invasion was tested on SF SU-ECM invasion substrates in the presence of 100 ng/mL PHSRN peptide and increasing concentrations of blocking COMY-4A2 anti–MMP-1 mAb (29). As shown in Fig. 4*A*, the anti–MMP-1 mAb was equally effective at blocking PHSRN-induced invasion by all four cell types. Complete inhibition of invasion was achieved by a concentration of 100 to 300 μg/mL, whereas the isotype control antibody (300 μg/mL) failed to significantly affect invasion. In contrast to the role of MMP-1, results of invasion assays using inhibitory anti–MMP-2 (CA-4001) and anti–MMP-9 (GE-213) mAbs (30, 31) suggested that neither MMP-2 nor MMP-9 activities function in PHSRN-induced invasion of SU-ECM, although zymography of SF media from PHSRN-treated and untreated MCF-10A, SUM-52 PE, and SUM-149 PT cells shows that all of these cell lines secrete activated forms of both MMP-2 and MMP-9 and that the levels of both gelatinases are unchanged by exposure to the PHSRN peptide (data not shown). The anti–MMP-1 mAb was also equally effective at inhibiting serum-induced invasion by SUM-52 PE and SUM-149 PT cells (Fig. 4*B*). Although SUM-52 PE and SUM-149 PT cells, as well as MCF-10A cells, secrete abundant MMP-2 and MMP-9 in the presence of serum (data not shown), insignificant inhibition of serum-induced invasion was observed with high concentrations of the anti–MMP-2 and anti–MMP-9 mAbs. Thus, these data demonstrate that MMP-1 also functions specifically in serum-induced invasion by SUM-149 PT and SUM-52 PE cells. Furthermore, the specific role of MMP-1 in serum-induced invasion was also confirmed for HME and MCF-10A mammary epithelial cells because increasing concentrations of anti–MMP-1 mAb reduced anti $\alpha_4\beta_1$-induced invasion, whereas anti–MMP-2 and anti–MMP-9 mAbs had no significant effect (Fig. 4*C*).

Stimulation of Matrix Metalloproteinase-1 Accumulation by the PHSRN Peptide. Adherent, SF breast cancer and mammary epithelial cells were treated with PHSRN and/or LDV peptides, and the cells were lysed, immunoblotted, and probed with anti–MMP-1 rabbit antiserum to compare the levels of cell-associated MMP-1. Immunoblots were run four times for each cell type, and relative band densities were determined for each treatment. Nearly all MMP-1 appeared to migrate in a single band of M_r 52,000, suggesting that cell-associated MMP-1 is predominantly the latent form. Mean MMP-1 band densities with first SDs are shown in $A-C$ of Fig. 5, as follows: Fig. 5*A*, MCF-10A; Fig. 5*B*, SUM-52 PE; and Fig. 5*C*, SUM-149 PT. As shown in Fig. 5*A*, PHSRN stimulated MMP-1 accumulation in MCF-10A cells, whereas equimolar LDV peptide did not. However, when mixed with the PHSRN peptide, LDV blocked the accumulation of MMP-1, whereas the scrambled LDV peptide failed to reduce PHSRN-induced MMP-1 accumulation. These results are consistent with the reported role of the $\alpha_4\beta_1$ receptor in fibroblasts (15). Moreover, consistent with the lack of surface $\alpha_4\beta_1$ expression in SUM-52 PE and SUM-149 PT cells, the LDV peptide had no inhibitory effect on PHSRN-induced MMP-1 accumulation in these breast cancer cells (Fig. 5*B* and *C*). Fig. 5*D* shows an example of a typical blot used for this analysis.

Although MMP-1 has been shown to associate with surface $\alpha_2\beta_1$ integrin collagen receptor to achieve activation and facilitate migration on collagen (35) and would thus be detectable in cell lysates, MMP-1 should also be secreted into the media of adherent cell

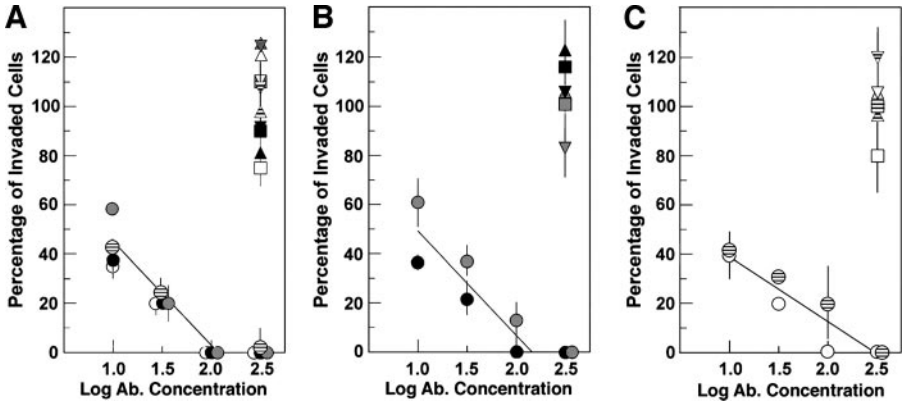

Fig. 4. Inhibition of $\alpha_5\beta_1$-induced invasion by blocking anti–MMP-1 mAb. *A*, inhibition of Ac-PHSRN-NH_2–induced invasion. *B*, inhibition of FCS-induced invasion. *C*, inhibition of P4C2-induced invasion. *X axes*, log antibody concentration (in μg/mL). *Y axes*, mean percentages of invasive cells, relative to the mean percentages of invasive cells in the absence of antibody. ●, SUM-149 PT cells in COMY-4A2 blocking anti–MMP-1 mAb; ○, SUM-52 PE cells in COMY-4A2 mAb; ⊜, MCF-10A cells in COMY-4A2 mAb; ○, HME cells in COMY-4A2 mAb. ■, SUM-149 PT cells in isotype control antibody; ▨, SUM-52 PE cells in isotype control antibody; □, HME cells in isotype control antibody; ▤, MCF-10A in isotype control antibody. ▲, SUM-149 PT cells in CA-4001 blocking anti–MMP-2 mAb; △, SUM-52 PE cells in CA-4001 blocking anti–MMP-2 mAb; ⧋, MCF-10A cells in CA-4001 blocking anti–MMP-2 mAb; △, HME cells in CA-4001 blocking anti–MMP-2 mAb. ▼, SUM-149 PT cells in GE-213 blocking anti–MMP-9 mAb; ▽, SUM-52 PE cells in GE-213 blocking anti–MMP-9 mAb; ⧩, MCF-10A cells in GE-213 blocking anti–MMP-9 mAb; ▽, HME cells in GE-213 blocking anti–MMP-9 mAb.

cultures treated with the PHSRN peptide. To test whether PHSRN treatment could cause a rapid increase in both the latent and activated forms of MMP-1 in the medium, adherent SF cultures of MCF-10A, SUM-52 PE, and SUM-149 PT cells were treated for 1 hour to 6 hours with the PHSRN peptide or were left untreated. All treated and untreated cultures were run in triplicate. Media from PHSRN-treated and untreated cultures were concentrated, and equal volumes of the concentrated media from each sample were analyzed by immunoblotting for the presence of MMP-1. As shown in Fig. 6*A*, 2 hours of PHSRN treatment induced significant increases in the mean levels of both latent and activated MMP-1 in the media from adherent MCF-10A, SUM-52 PE, and SUM-149 PT cells, relative to the amounts

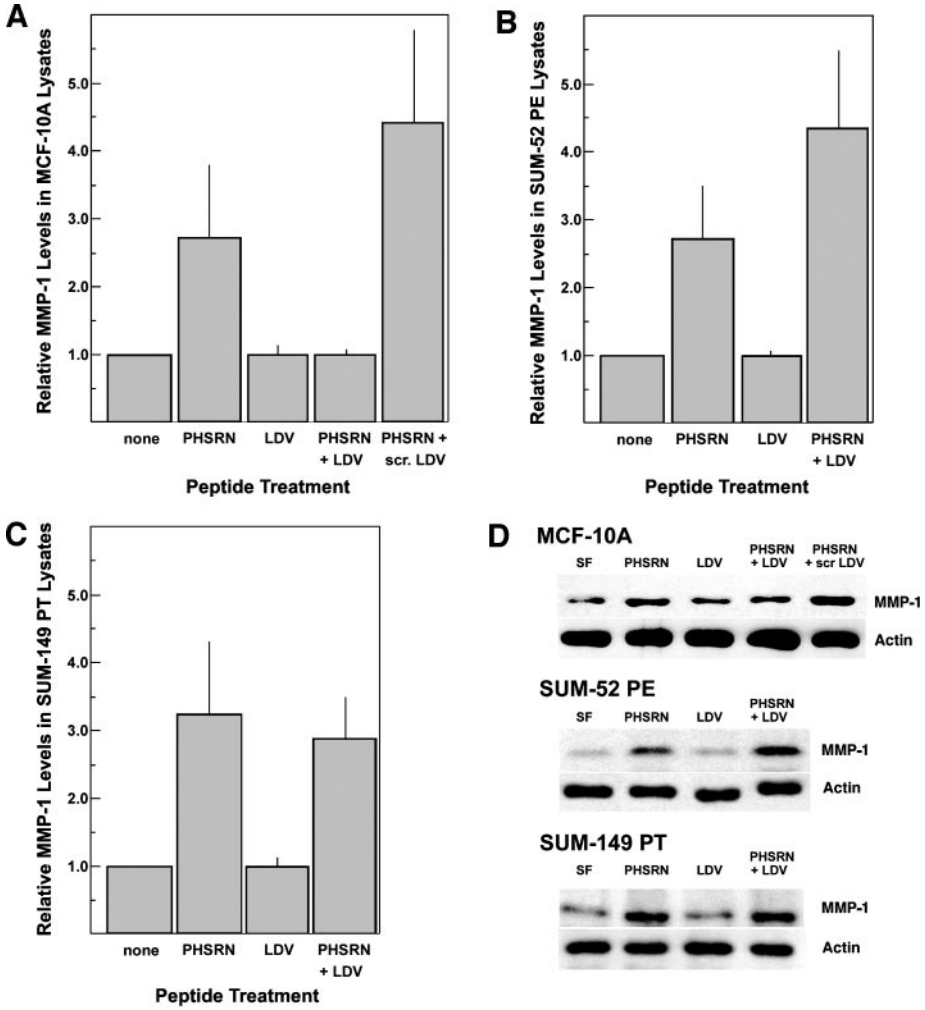

Fig. 5. The $\alpha_5\beta_1$ and $\alpha_4\beta_1$ peptide ligands control the levels of MMP-1 in cell lysates. *A*, MCF-10A. *X axis*, peptide treatment; *Y axis*, relative MMP-1 levels in MCF-10A lysates. Means with first SDs are shown. *B*, SUM-52 PE. *X axis*, peptide treatment; *Y axis*, relative MMP-1 levels in SUM-52 PE lysates. Means with first SDs are shown. *C*, SUM-149 PT. *X axis*, peptide treatment; *Y axis*, relative MMP-1 levels in SUM-149 PT lysates. Means with first SDs are shown. *D*, example of a MMP-1 immunoblot, performed on the lysates of treated cells, as labeled. *SF*, no peptide; *PHSRN*, 1 μg/mL Ac-PHSRN-NH_2 (SF medium); *LDV*, 2.5 μg/mL Ac-LHGPEILD-VPST-NH_2 (SF medium); *PHSRN + LDV*, 1 μg/mL Ac-PHSRN-NH_2 and 2.5 μg/mL Ac-LHGPEILDVPST-NH_2 (SF medium); *PHSRN + scr LDV*, 1 μg/mL Ac-PHSRN-NH_2 and 2.5 μg/mL Ac-Ac-PGVLSEHPTLID-NH_2 (SF medium). Equal amounts of protein were loaded in each well of the gel as indicated by the actin loading controls shown below the MMP-1 lanes in each panel.

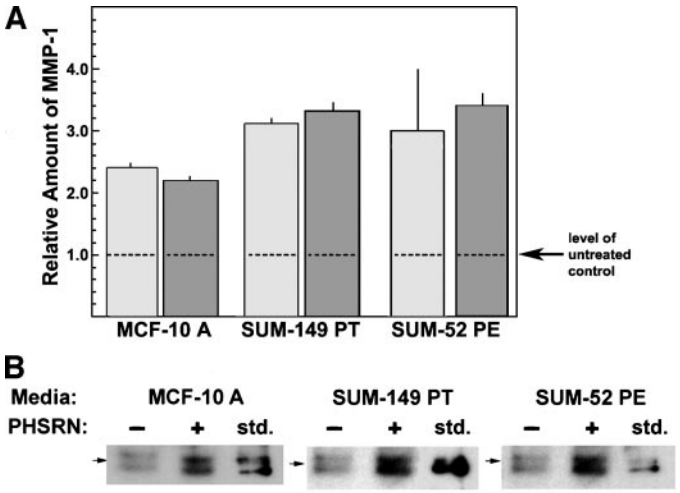

Fig. 6. The PHSRN peptide Ac-PHSRN-NH_2 induces increased levels of both latent and activated MMP-1 in the SF media of adherent MCF-10A, SUM-52 PE, and SUM-149 PT cells. *A*, amounts of latent and activated MMP-1 in equal volumes (40 μL) of concentrated media from PHSRN-treated, adherent cultures, relative to the amounts from untreated cultures. *X axis*, cell types; *Y axis*, relative amount of MMP-1. □, latent MMP-1. ■, activated MMP-1. *Dotted line* indicates the relative MMP-1 level in untreated controls. *B*, examples of MMP-1 bands on immunoblots of PHSRN-treated and untreated SF media from adherent cultures of MCF-10A, SUM-149 PT, and SUM-52 PE cells. Media: *MCF-10 A*, media from MCF-10A cells; *SUM-52 PE*, media from SUM-52 PE cells; *SUM-149 PT*, media from SUM-149 PT cells. PHSRN: +, media from cells treated with Ac-PHSRN-NH_2 at a concentration of 1 μg/mL per 20,000 cells; −, media from parallel cultures of untreated cells; *std.*, purified MMP-1 standard. The position of the M_r 50,000 marker is indicated on each panel (*arrow*).

secreted by untreated cells. Fig. 6*B* compares examples of the M_r 52,000 and M_r 43,000 MMP-1 bands from PHSRN-treated and untreated MCF-10A, SUM-149 PT, and SUM-52 PE cells. The PHSRN-induced up-regulation of two anti–MMP-1 antibody-reactive proteins, a M_r 52,000 latent form and a form exhibiting a M_r 9,000–10,000 reduction, is illustrated. Moreover, the observed molecular weights are consistent with those reported for latent MMP-1 (M_r 52,000) and activated MMP-1 (M_r 43,000; ref. 36). Also, as shown in Fig. 6, both bands comigrated with the purified MMP-1 standards run on each gel. For each cell type, maximal levels of latent and activated MMP-1 were observed after 2 hours of treatment, and then they began to decline (data not shown).

Stimulation of Matrix Metalloproteinase-1 Activity by the PHSRN Peptide. MMP-1 activity levels were monitored in media of adherent cultures of MCF-10A, SUM-52 PE, and SUM-149 PT cells for up to 6 hours after the initiation of PHSRN treatment. As shown in Fig. 7*A*, activity reached a maximum in about 2 hours and then started to decline toward the control level after 4 hours. Differences in MMP-1 activity between PHSRN-treated cells and untreated cells incubated in parallel were highly significant ($P_0 < 0.0001$). Also, the time of peak MMP-1 activity corresponded with the time of maximal MMP-1 levels in the medium, as assayed by immunoblotting (Fig. 6; data not shown). As shown in Fig. 7*B*, temporal changes in MMP-1 activity were also well correlated with the PHSRN-induced invasion time courses of these cell lines on SU-ECM invasion substrates. Furthermore, suspension and placement on SU-ECM for identical periods of time, without exposure to PHSRN peptide, resulted in no detectable invasion by any of the cell lines.

DISCUSSION

We report that a peptide consisting of the PHSRN sequence of fibronectin induces rapid, $\alpha_5\beta_1$-mediated invasion by normal and immortalized mammary epithelial cells, as well as by metastatic breast cancer cells. Although the intact fibronectin of serum does not induce mammary epithelial cell invasion, due to $\alpha_4\beta_1$ expression, invasion is induced if $\alpha_4\beta_1$ is inhibited with a blocking antibody. Furthermore, $\alpha_4\beta_1$ repression of $\alpha_5\beta_1$-mediated invasion occurs if PHSRN-treated mammary epithelial cells are also exposed to a peptide consisting of the LDV sequence (34) of the fibronectin connecting segment. Moreover, in SF breast cancer cells lacking $\alpha_4\beta_1$ on their surfaces, the LDV peptide fails to repress PHSRN-induced invasion. These results are consistent with the down-regulation of $\alpha_4\beta_1$ on the surfaces of invasive breast cancer cells as well as in transformed mammary epithelial cells overexpressing the ERBB-2 oncogene (19) and in prostate cancer cells (18). They suggest that $\alpha_4\beta_1$ functions to regulate $\alpha_5\beta_1$-mediated invasion and that the loss of surface $\alpha_4\beta_1$ may be an important event in the development of the invasive phenotype in cancer.

We also found, through the use of blocking anti–MMP-1, anti–MMP-2, and anti–MMP-9 mAbs, that PHSRN- and serum-induced invasion of basement membranes by mammary epithelial cells and breast cancer cells appears to be a MMP-1–dependent process. Consistent with the apparent dependence of invasion on MMP-1, it was also observed that PHSRN treatment induces a rapid increase in both cell-associated and secreted MMP-1 protein, as well as in MMP-1 activity in the medium. Furthermore, PHSRN-induced MMP-1 accumulation in mammary epithelial cells, but not in breast cancer cells, is prevented by the LDV peptide ligand of $\alpha_4\beta_1$ integrin. Also, the rapid increase in PHSRN-induced MMP-1 activity closely parallels that of basement membrane invasion. A similarly rapid induction of MMP-1 expression has also been observed in osteoblasts treated with platelet-derived growth factor (37). Thus, MMP-1 may play an important role in $\alpha_5\beta_1$-mediated invasion in breast cancer cells, and its up-regulation is likely a consequence of reduced levels of surface $\alpha_4\beta_1$ fibronectin receptor relative to mammary epithelial cells. Because reduced levels of surface $\alpha_4\beta_1$ integrin also give rise to $\alpha_5\beta_1$-mediated, serum-dependent invasiveness in prostate cancer (6), this could be a general mechanism contributing to metastasis.

MMPs carry out most of the connective tissue destruction associ-

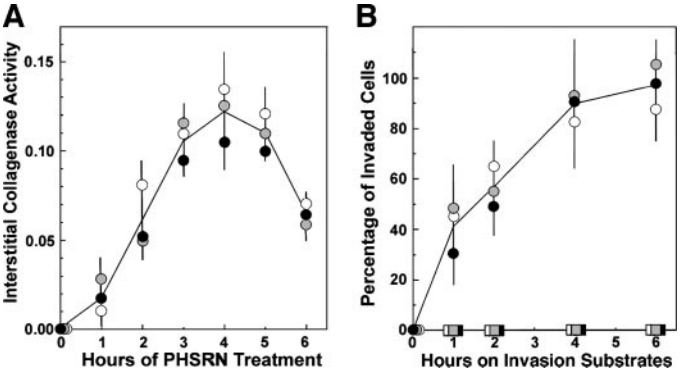

Fig. 7. PHSRN up-regulates MMP-1 activity in parallel with the PHSRN-induced cell invasion capacity. *A*, quantitation of MMP-1 activity in media of adherent cultures of SUM-52 PE, SUM-149 PT, and MCF-10A cells that were treated with Ac-PHSRN-NH_2. *X axis*, hours of treatment with Ac-PHSRN-NH_2. *Y axis*, concentration of active interstitial collagenase MMP-1 (ng/mL), as interpolated from a standard curve. Background MMP-1 levels in untreated cells were as follows: *MCF-10A*, 0.21 ng/mL; *SUM-52 PE*, 0.22 ng/mL; and *SUM-149 PT*, 0.23 ng/mL. These values were subtracted from the points plotted. ●, SUM-149 PT cells; ⊜, SUM-52 PE cells; ○, MCF-10A cells. Means and first SDs are shown. *B*, time course of Ac-PHSRN-NH_2–induced invasion of SUM-149 PT, SUM-52 PE, and MCF-10A cells. *X axis*, hours on SU-ECM invasion substrates. *Y axis*, mean percentage of invasive cells, relative to the percentages of invasive cells after 24 hours. ●, SF SUM-149 PT cells treated with 1 μg/mL Ac-PHSRN-NH_2; ⊜, SF SUM-52 PE cells treated with 1 μg/mL Ac-PHSRN-NH_2; ○, SF MCF-10A cells treated with 1 μg/mL Ac-PHSRN-NH_2. ■, SF SUM-149 PT cells in 0 μg/mL Ac-PHSRN-NH_2; ▨, SF SUM-52 PE cells in 0 μg/mL Ac-PHSRN-NH_2; □, SF MCF-10A cells in 0 μg/mL Ac-PHSRN-NH_2. Means and first SDs are shown.

ated with cancer invasion and metastasis (reviewed in ref. 38). Zymography, immunoblotting, and immunohistochemistry have demonstrated increased levels of MMPs and MMP activities in human breast cancer, relative to normal breast tissues (39). However, the role of interstitial collagenases in tumor invasion and metastasis has only recently been appreciated. It has been suggested that collagenase expression is a marker for tumor progression in breast cancer, as well as in many other types of cancers (40, 41). Zymography of human breast carcinomas and normal breast tissues has also shown significant MMP-1 levels in most invasive cancers, in contrast to normal breast tissues (42). Immunohistochemistry of sectioned, invasive breast tumors and their surrounding tissues has also shown a significant correlation of MMP-1 expression with tumor stage (39). Furthermore, in most invasive breast carcinomas, *in situ* hybridization has demonstrated high levels of MMP-1 transcripts in both breast cancer cells and stromal cells at their invasive fronts (43). In fact, MMP-1 is also up-regulated in human breast cancer cells cocultured with fibroblasts (44), suggesting that direct interactions between these two cell types can lead to increased collagenase expression in breast cancer. In contrast, although MMP-2 transcripts have been found at high levels in invasive breast carcinomas, MMP-2 mRNA is also up-regulated in preinvasive lesions, suggesting that MMP-1 is specifically up-regulated as breast cancers become invasive (43). Interestingly, it has also been shown that interstitial collagenase also cleaves entactin, thus contributing directly to the degradation of basement membrane and hence potentially contributing to the transiting of epithelial barriers by tumor cells (45), in addition to stromal proteolysis.

In other cancers, such as colon and esophageal cancers, immunohistochemical detection of MMP-1 expression is also associated with increased invasive potential and poor prognosis (46, 47). Moreover, increased MMP-1 expression in tumor cells is significantly correlated with the depth of tumor invasion, angiogenesis, lymphangiogenesis, and the presence of local and distant metastases (48). Also, a transcription-enhancing point mutation in the MMP-1 gene promoter, which correlates with MMP-1 overexpression in tumor cells, is associated with increased malignancy in breast and lung cancer (49, 50). Thus, whereas many MMPs contribute to tumor angiogenesis and metastasis, interstitial collagenase may be critical for the development of the invasive phenotype during cancer progression.

REFERENCES

1. Geiger B, Bershadsky A, Pankov R, Yamada KM. Transmembrane crosstalk between the extracellular matrix-cytoskeleton crosstalk. Nat Rev Mol Cell Biol 2001;2:793–805.
2. Danen EH, Yamada KM. Fibronectin, integrins, and growth control. J Cell Physiol 2001;189:1–13.
3. Livant DL, Brabec RK, Kurachi K, et al. The PHSRN sequence induces extracellular matrix invasion and accelerates wound healing in obese diabetic mice. J Clin Investig 2000;105:1537–45.
4. White ES, Livant DL, Markwart S, Arenberg DA. Monocyte-fibronectin interactions, via alpha(5)beta(1) integrin, induce expression of CXC chemokine-dependent angiogenic activity. J Immunol 2001;167:5362–6.
5. Brakebusch C, Bouvard D, Stanchi F, Sakai T, Fassler R. Integrins in invasive growth. J Clin Investig 2002;109:999–1006.
6. Livant DL, Brabec RK, Pienta KJ, et al. Anti-invasive, antitumorigenic, and antimetastatic activities of the PHSCN sequence in prostate carcinoma. Cancer Res 2000;60:309–20.
7. van Golen KL, Bao L, Brewer GJ, et al. Suppression of tumor recurrence and metastasis by a combination of the PHSCN sequence and the antiangiogenic compound tetrathiomolybdate in prostate carcinoma. Neoplasia 2002;4:373–9.
8. Yamada KM. Fibronectin peptides in cell migration and wound repair. J Clin Investig 2000;105:1507–9.
9. Gibson AW, Burke RD. Migratory and invasive behavior of pigment cells in normal and animalized sea urchin embryos. Exp Cell Res 1987;173:546–57.
10. Livant DL, Linn S, Markwart S, Shuster J. Invasion of selectively permeable sea urchin embryo basement membranes by metastatic tumor cells, but not by their normal counterparts. Cancer Res 1995;55:5085–93.
11. Noel AC, Calle A, Emonard HP, et al. Invasion of reconstituted basement membrane matrix is not correlated to the malignant metastatic cell phenotype. Cancer Res 1991;51:405–14.
12. Amemiya S. Development of the basal lamina and its role in migration and pattern formation of primary mesenchyme cells in sea urchin embryos. Dev Growth Differ 1989;31:131–45.
13. McCarthy RA, Beck K, Burger MM. Laminin is structurally conserved in the sea-urchin basal lamina. EMBO J 1987;6:1587–93.
14. Solursh M, Katow H. Initial characterization of sulfated macromolecules in the blastocoels of mesenchyme blastulae of Strongylocentrotus-purpuratus and Lytechinus-pictus. Dev Biol 1982;94:326–36.
15. Huhtala P, Humphries MJ, McCarthy JB, et al. Cooperative signaling by alpha 5 beta 1 and alpha 4 beta 1 integrins regulates metalloproteinase gene expression in fibroblasts adhering to fibronectin. J Cell Biol 1995;129:867–79.
16. Grinnell F, Zhu M. Identification of neutrophil elastase as the proteinase in burn wound fluid responsible for degradation of fibronectin. J Investig Dermatol 1994; 103:155–61.
17. Greiling D, Clark RA. Fibronectin provides a conduit for fibroblast transmigration from collagenous stroma into fibrin clot provisional matrix. J Cell Sci 1997;110: 861–70.
18. Rokhlin OW, Cohen MB. Expression of cellular adhesion molecules on human prostate tumor cell lines. Prostate 1995;26:205–12.
19. Ignatoski KM, Maehama T, Markwart SM, et al. ERBB-2 overexpression confers PI 3′ kinase-dependent invasion capacity on human mammary epithelial cells. Br J Cancer 2000;82:666–74.
20. Mosher DF. Physiology of fibronectin. Annu Rev Med 1984;35:561–75.
21. Ruoslahti E, Hayman EG, Pierschbacher M, Engvall E. Fibronectin: purification, immunochemical properties, and biological activities. Methods Enzymol 1982;82: 803–31.
22. Ethier SP, Mahacek ML, Gullick WJ, Frank TS, Weber BL. Differential isolation of normal luminal mammary epithelial cells and breast cancer cells from primary and metastatic sites using selective media. Cancer Res 1993;53:627–35.
23. Ignatoski KM, Ethier SP. Constitutive activation of pp125fak in newly isolated human breast cancer cell lines. Breast Cancer Res Treat 1999;54:173–82.
24. Atherton E, Sheppard RC. Solid phase peptide synthesis: a practical approach. Oxford, United Kingdom: IRL Press; 1989.
25. Wayner EA, Carter WG, Piotrowicz RS, Kunicki TJ. The function of multiple extracellular matrix receptors in mediating cell adhesion to extracellular matrix: preparation of monoclonal antibodies to the fibronectin receptor that specifically inhibit cell adhesion to fibronectin and react with platelet glycoproteins Ic-IIa. J Cell Biol 1988;107:1881–91.
26. Carter WG, Wayner EA, Bouchard TS, Kaur P. The role of integrins alpha 2 beta 1 and alpha 3 beta 1 in cell-cell and cell-substrate adhesion of human epidermal cells. J Cell Biol 1990;110:1387–404.
27. Wayner EA, Garcia-Pardo A, Humphries MJ, McDonald JA, Carter WG. Identification and characterization of the T lymphocyte adhesion receptor for an alternative cell attachment domain (CS-1) in plasma fibronectin. J Cell Biol 1989;109:1321–30.
28. Wayner EA, Gil SG, Murphy GF, Wilke MS, Carter WG. Epiligrin, a component of epithelial basement membranes, is an adhesive ligand for alpha 3 beta 1 positive T lymphocytes. J Cell Biol 1993;121:1141–52.
29. Birkedal-Hansen B, Moore WG, Taylor RE, Bhown AS, Birkedal-Hansen H. Monoclonal antibodies to human fibroblast procollagenase. Inhibition of enzymatic activity, affinity purification of the enzyme, and evidence for clustering of epitopes in the NH2-terminal end of the activated enzyme. Biochemistry 1988;27:6751–8.
30. Fridman R, Fuerst TR, Bird RE, et al. Domain structure of human 72-kDa gelatinase/type IV collagenase. Characterization of proteolytic activity and identification of the tissue inhibitor of metalloproteinase-2 (TIMP-2) binding regions. J Biol Chem 1992; 267:15398–405.
31. Schnaper HW, Grant DS, Stetler-Stevenson WG, et al. Type IV collagenase(s) and TIMPs modulate endothelial cell morphogenesis in vitro. J Cell Physiol 1993;156: 235–46.
32. Aota S, Nomizu M, Yamada KM. The short amino acid sequence Pro-His-Ser-Arg-Asn in human fibronectin enhances cell-adhesive function. J Biol Chem 1994;269: 24756–61.
33. Altroff H, van der Walle CF, Asselin J, et al. The eight FIII domain of human fibronectin promotes integrin alpha5beta1 binding via stabilization of the ninth FIII domain. J Biol Chem 2001;276:38885–92.
34. Komoriya A, Green LJ, Mervic M, et al. The minimal essential sequence for a major cell type-specific adhesion site (CS1) within the alternatively spliced type III connecting segment domain of fibronectin is leucine-aspartic acid-valine. J Biol Chem 1991;266:15075–9.
35. Dumin JA, Dickeson SK, Stricker TP, et al. Pro-collagenase-1 (matrix metalloproteinase-1) binds the alpha(2)beta(1) integrin upon release from keratinocytes migrating on type I collagen. J Biol Chem 2001;276:29368–74.
36. Birkedal-Hansen H, Moore WGI, Bodden MK, et al. Matrix metalloproteinases: a review. Crit Rev Oral Biol Med 1993;4:197–250.
37. Varghese S, Delany AM, Liang L, et al. Transcriptional and posttranscriptional regulation of interstitial collagenase by platelet-derived growth factor BB in bone cell cultures. Endocrinology 1996;137:431–7.
38. Curran S, Murray GI. Matrix metalloproteinases in tumour invasion and metastasis. J Pathol 1999;189:300–8.
39. Garbett EA, Reed MW, Stephenson TJ, Brown NJ. Proteolysis in human breast cancer. Mol Pathol 2000;53:99–106.
40. Nakopoulou L, Giannopoulou I, Gakiopoulou H, et al. Matrix metalloproteinase-1 and -3 in breast cancer: correlation with progesterone receptors and other clinicopathologic features. Hum Pathol 1999;30:436–42.

41. Brinckerhoff CE, Rutter JL, Benbow U. Interstitial collagenases as markers of tumor progression. Clin Cancer Res 2000;6:4823–30.
42. Remacle AG, Noel A, Duggan C, et al. Assay of matrix metalloproteinases types 1, 2, 3 and 9 in breast cancer. Br J Cancer 1998;77:926–31.
43. Brummer O, Athar S, Riethdorf L, Loning T, Herbst H. Matrix-metalloproteinases 1, 2, and 3 and their tissue inhibitors 1 and 2 in benign and malignant breast lesions: an in situ hybridization study. Virchows Arch 1999;435:566–73.
44. Ito A, Nakajima S, Sasaguri Y, Nagase H, Mori Y. Co-culture of human breast adenocarcinoma MCF-7 cells and human dermal fibroblasts enhances the production of matrix metalloproteinases 1, 2 and 3 in fibroblasts. Br J Cancer 1995;71:1039–45.
45. Sires UI, Griffin GL, Broekelmann TJ, et al. Degradation of entactin by matrix metalloproteinases. Susceptibility to matrilysin and identification of cleavage sites. J Biol Chem 1993;268:2069–74.
46. Murray GI, Duncan ME, O'Neil P, Melvin WT, Fothergill JE. Matrix metalloproteinase-1 is associated with poor prognosis in colorectal cancer. Nat Med 1996;2:461–2.
47. Murray GI, Duncan ME, O'Neil P, et al. Matrix metalloproteinase-1 is associated with poor prognosis in oesophageal cancer. J Pathol 1998;185:256–61.
48. Shiozawa J, Ito M, Nakayama T, et al. Expression of matrix metalloproteinase-1 in human colorectal carcinoma. Mod Pathol 2000;13:925–33.
49. Rutter JL, Mitchell TI, Buttice G, et al. A single nucleotide polymorphism in the matrix metalloproteinase-1 promoter creates an Ets binding site and augments transcription. Cancer Res 1998;58:5321–5.
50. Zhu Y, Spitz MR, Lei L, Mills GB, Wu X. A single nucleotide polymorphism in the matrix metalloproteinase-1 promoter enhances lung cancer susceptibility. Cancer Res 2001;61:7825–9.